JOURNAL OF THE KOREAN ASTRONOMICAL SOCIETY
39: 51 ~ 56, 2006

DEVELOPMENT OF SEMI-VLBI SYSTEM AND OBSERVATION OF SUN AT 21 cm

YONG-SUN PARK[1], HYUN WOO KANG[1], HYOUK KIM[2], HEUI-JEONG KANG[2], MYEONG-KEUN JEE[2], SUL-GI LEE[2], JUNG-HYUN AHN[2], JIN-SU KIM[3], YOUNG-SOO SHIN [3], AND SONG-HUN KANG[4]
[1] FPRD, School of Physics and Astronomy, SNU, Seoul, Korea
E-mail: yspark@astro.snu.ac.kr
[2] Gyeonggi Science High School, Suwon, Korea
[3] School of Earth and Environmental Sciences, SNU, Seoul, Korea
[4] Korea Advanced Institute of Science and Technology, Daejon, Korea
(Received May 24, 2006; Accepted June 1, 2006)

ABSTRACT

We report the development of a semi-VLBI observation system operating at 21 cm and present the measurement of visibility function toward the sun using this system. The system consists of two 2.3 meter antennas with a maximum separation of 35 meter, a conventional high speed data acquisition system, and a set of programs for software correlation. Since two local oscillators of receiver modules are independent, data had to be fringe-fitted to yield the visibility amplitude. It is found that the visibility amplitude decreases and then bounces back as baseline increases. We confirm that solar disk with brighter limb best explains the measured visibility amplitude.

Key words : instrumentation: interferometer — Sun: general — Sun: radio radiation — radio continuum: general

I. INTRODUCTION

Since radio observation suffers from poor resolution compared to optical one, it was quite evident from the beginning of radio astronomy that it is necessary to develop interferometry technique or its extension - the so-called VLBI. Nowadays the interferometry technique becomes popular and extends into near IR and optical astronomy (eg. ALMA and VLTI). Despite these importance, access to interferometer systems has been very limited even to professional researchers. Moreover, difficulties in understanding the theory and operational principle of interferometry seem to be common sense.

In an attempt to make the interferometer system easily accessable to (under-)graduate students possibly including high school ones, and to help to understand how the interferometer works, we constructed a two-element interferometer operating at 1.4GHz, and made observations toward the sun using this system. Though it is mainly for educational purpose, it could also be used for science research of, at least, the sun, if more antennas are combined, since solar radio radiation is strong enough, this frequency is not monitored continuously by any existing systems, and new phenomena like 'microbursts' seem to occur occasionally with various life time (Bastian 1991).

In order to minimize mechanical and electronical work, we allowed local oscillator (LO) to run seperately and decided to correlate data by software, which is actually the strategy that modern VLBI pursues. Therefore, this system involves many modern aspects of VLBI. However, the outputs of antennas are fed into a common data aqusition card in a PC, and thus the synchronization of data logging is achieved automatically. In this respect, we will call this 'semi-VLBI' system.

Since the LO frequencies can not be exactly the same each other, fringe fitting process is needed to derive visibility function. With crystal oscillator used as the frequency standard of LO, the maximum coherence time of the system will be around 10^3 seconds, which is roughly estimated from its Allan variance (Thompson et al. 1986). This is much longer than typical data aquisition time of $0.1 - 0.2$ seconds, but may be shorter than the time required for whole observing session lasting a few hours at least. Moreover sources for phase calibration are not available. Therefore we will work with the visibility amplitude only, instead of deriving both phase and amplitude.

II. DEVELOPMENT OF SEMI-VLBI SYSTEM

(a) Construction of Telescopes

The radio telescope with 2.3 meter in diameter was designed mainly for single dish mode operation by Haystack observatory and manufactured by CASS Inc. Detailed information on this telescope is available at http://haystack.mit.edu/edu/undergrad/srt/index.html. The F/D ratio of main reflector is 0.375 and metal mesh is used for reflecting surface. A pair of telescopes were assembled and installed at Gyeonggi science high school, Suwon, Korea, as shown in Fig. 1. One is fixed,

Corresponding Author: Y.-S. Park

but the other is movable, mounted on a cart, so that we can measure visibility function for various baselines. The maximum baseline length is approximately 200 λ.

Receiver module located at the prime focus receives and down-converts signals with image rejection mixer that selects signal from lower side band only. Typical system temperature is 100K. Since the sky is transparent at this frequency, the system temprature is contributed by receiver noise temperature and loss at the feed. A correlation chip in the receiver module calculates auto-correlation function to generate spetra when used in a single dish mode. For interferometry mode, we use intermediate frequency (IF) signal from video output port, taken before detection at the auto-correlation processing unit. The frequency range of this IF signal is 0.5 to 3 MHz.

Impedance matching pads are inserted between the receiver and data aqusisition card since the impedance of cable is 75 Ω, whereas that of the card is 50 Ω. We also add low pass filters with cutoff frequency of 2.5 MHz after the matching pad. This cutoff frequency is determined by the sampling speed of a data aquisition card and data file size (see next section). Typical IF pass band is shown in Fig. 2.

(b) Telescope Control and Data Acquisition

Source tracking and calculation of system temperature are carried out individually with the use of programs supplied by the telescope manufacturer.

We developed data taking system using a data acquisition card, DAQScope PCI-5102, and LabView made by National Instuments. Signals from the two telescopes are fed into this card. The LabView controls the sampling rate and input voltage range of the card and carries out auxilliary functions like displaying data as functions of time and frequency. The resolution is fixed to 8 bits and the data taking is carried out simultaneously for the two channels.

The maximum sampling rate of the PCI-5102 card is 20 MHz, and thus the bandwidth of signals can be as wide as 10 MHz. Wider bandwidth guarantees better S/N, but the generation of prohibitably large number of data prevents data reduction from being processed in a reasonable time scale. As a compromise, we set the sample rate to 6.67 MHz and the number of data per session to one million. Therefore the total integration time is 0.15 seconds per session. The size of a data file amounts to 10 MBytes with these observation parameters.

(c) Software Correlator

Several simple FORTRAN programs are written for data reduction. Their aims are to find fringe for various delays, to calculate power spectra, to derive visibility amplitude, and to calculate baseline vectors in the u-v plane. Though they are rather short in length, they replace hardware correlators with much less cost and

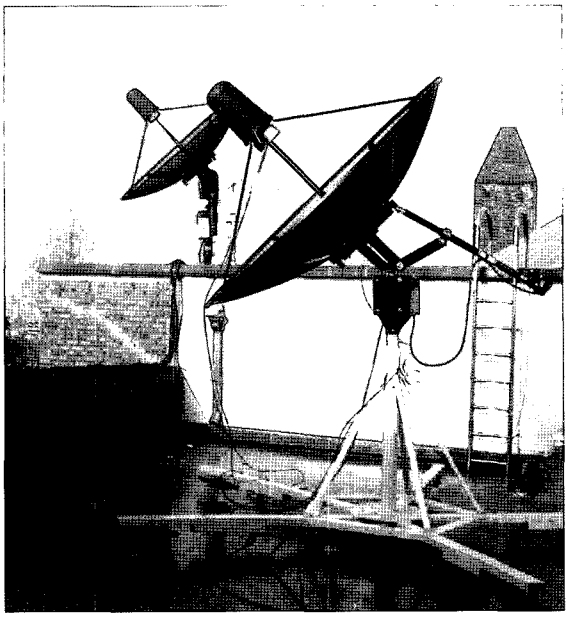

Fig. 1.— Semi-VLBI system composed of two small an tennas

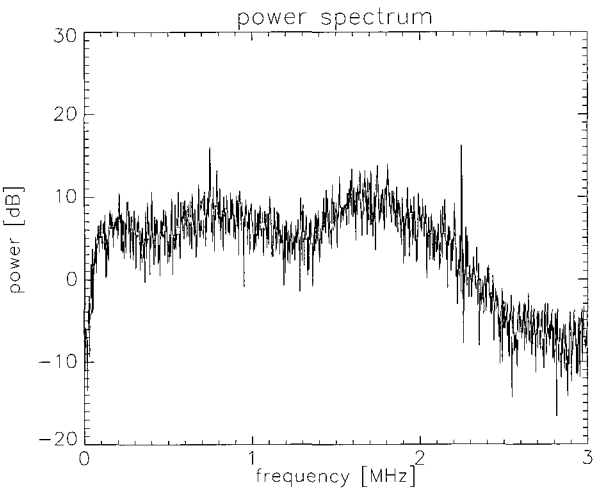

Fig. 2.— Typical IF pass band is shown. Radio interfer ence is noted at a few frequencies.

behave like *lens* of optical telescope.

III. TEST OF SEMI-VLBI SYSTEM

Before deriving reliable visibility function, we tested the performance of the system and investigated peripheral conditions like radio frequency interference (RFI) by artificial sources nearby.

(a) Identification of Different Local Oscillator Frequencies

Since the frequency of LOs is different, simple cross-correlation of signals from the two telescopes will result in null visibility. Before correlation, we need to correct the frequency difference, which is known as fringe-fitting. In order to measure the amount of frequency difference, we inject monochromatic wave or CW to the two receivers. The frequency difference observed at IF band is found to be 12.1 KHz with a 3 % peak-to-peak variation. Since the frequencies of LOs change from time to time depending on the performance of phase lock loop inside the receiver module and on the outside condition such as ambient temperature, one can not use this fixed value, but needs to derive it from the measured data itself.

(b) Effect of Interference

In Fig. 2, one can note a few radio interferences. They can come either from the radio frequency (RF) band or directly from the IF band. All the interferences are close to CW and, if the artificial signals from a common origin are recorded, they can result in false correlation. In order to test this effect, we generated a new signal from a measured data set using a band pass filter function of LabView so that the new data set is free from interference. The center frequency and bandwidth of the filter function are 1.5 MHz and 1 MHz, respectively. The correlation of this data set is compared with the one without filtering. This comparison suggests that the cross-correlation is not affected by the interference. The RFI seems to be rather weak in power than the signal coming from the sun. We decided to use the data as they are, based on this results.

IV. OBSERVATION AND FRINGE FITTING

(a) Observation

After verifying the system performance with the various preliminary tests, we started observation and recorded data 14th and 28th April, 2006. Since there may be solar activities with various time scales, we avoid mixing data taken different days, and use the data of 28th only.

We moved one antenna element to 6 positions, baseline ranging from 4 m to 35 m. Data are taken two times toward the sun and once toward blank sky for calibration at each station. At the same time, we measured system temperature and antenna temperature of the sun in a single dish mode, which are also used for calibration. Since the system temperature is typically 100 K and the antenna temperature of the sun is 400K, noise is one quarter in power and one half in voltage.

Integration time is 0.15 seconds and the number of data is 10^6 per session. It took about a couple of hours to complete whole sessions. The system is found to be rather stable, since the output voltages remain constant with a 7 % of peak-to peak variation.

(b) Fringe Fitting

In order to correct the LO frequency difference, we first need to know the frequency difference using the recorded data. If the signal is monochromatic, it is easy to find it either by stretching or by compressing time axis of a data set from a telescope with respect to the other set and then by cross-correlating them. However, since the input signal has a bandwidth of 2.5 MHz, we need to consider other means to correct this effect.

Such signals from the two telescopes, $i = 1$ and 2, can be modeled as follows.

$$v_1(t) = \int A(\nu)\sin(2\pi\nu t + \phi(\nu))d\nu$$

and

$$v_2(t) = \int A(\nu)\sin(2\pi(\nu + \delta\nu)t + \phi(\nu))d\nu,$$

where the integration is effective only over the bandwidth of 0 to 2.5 MHz. We expand the latter one and compare it with the former one:

$$\begin{aligned} v_2(t) &= v_1(t)\cdot\cos(2\pi\delta\nu t) \\ &\quad + \int A(\nu)\cos(2\pi\nu t + \phi(\nu))d\nu \cdot \sin(2\pi\delta\nu t). \end{aligned}$$

We note that $v_2(t)$ resembles $v_1(t)$ when $\delta\nu t \simeq n$, but does $-v_1(t)$ when $\delta\nu t \simeq n + 1/2$. The contribution of the second term at the right hand side is negligible for these periods of time. If we multiply $v_1(t)$ and $v_2(t)$, then we will see the multiplied one changes its sign alternately on the average and the frequency of this modulation is just the LO frequency difference, $\delta\nu$. In order to see this more clearly, we selected one of data sets taken during experiment, averaged every 30 points of the multiplied data stream, and displayed it for various delays in Fig. 3.

From the figure, the frequency difference is estimated to be around 12.0515 KHz. During the one day session, the frequency difference ranged from 11.92 KHz to 12.23 KHz. Better way to see the frequency of this modulation is to Fourier transform data as shown in Fig. 4. Actually this could include other sources of frequency difference like different recording speed and Doppler shift when baseline is very long.

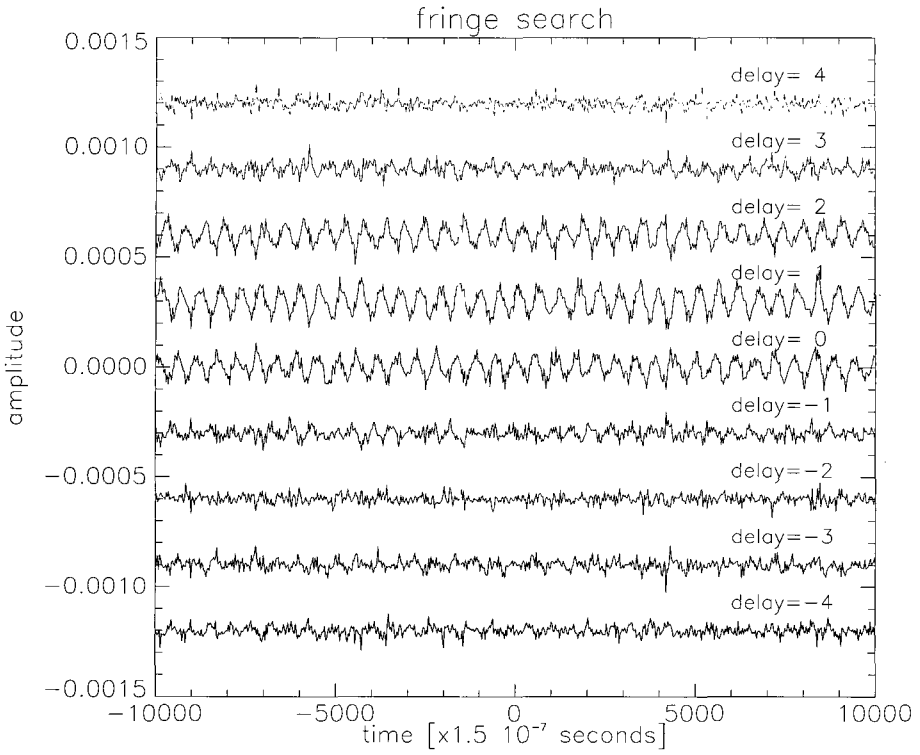

Fig. 3.— Examples of multiplication of two signals are displayed for various delays, where each data set is shifted arbitrarily for clarity. One point in the figure is an average of 30 data points. Delays are in unit of 1.5×10^{-7} seconds.

When this drift is noted, the way of calculating cross-correlation is that, for 3/8 of the modulation period of $1/\delta\nu$, both data are multipled normally, for next 1/8 cycle multiplication is skipped, and for next 3/8 cycle one side of the data stream changes sign and is multiplied by the other (Zensus et al. 1995). Then these multiplied data stream is averaged. Since the starting point of the cycle is not known a priori, the cross-correlation is serched for several values of the starting time of modulation. Since we are only interested in the amplitude of visibility, we also move back and forth one data set with respect to the other, to find maximum correlation value which is the amplitude of visibility function for a given baseline.

This process will make the calculated visibility amplitude smaller than true one. By using monochromatic signal, we can easily analytically compare the true visibility and the one calculated by the above mentioned method. The calculated one is smaller than the true one by a factor of $\sin(3\pi/8)/\pi = 1.70$. All the visibility amplitudes derived in this way are thus multipled by this value.

(c) Calibration

First we model the output voltage toward the sun as follows, taking noise into account.

$$V_{sun_1}(t) = G_1[v_{sun_1}(t) + v_{n_1}(t)]$$

and

$$V_{sun_2}(t) = G_2[v_{sun_2}(t) + v_{n_2}(t)],$$

where G_1 and G_2 are slowly varying conversion factors. The $v_{sun_i}(t)$ and $v_{n_i}(t)$ are signal from the sun and from the noise of telescope i, respectively. They are stationary stochastic variables with Gaussian distribution due to the finite bandwidth.

If we time-average the $V_{sun_1}(t)$ multiplied by $V_{sun_2}(t)$

$$\begin{aligned} P_{sun_{12}} &\equiv < V_{sun_1}(t) \cdot V_{sun_2}(t) > \\ &= G_1 G_2 < v_{sun_1}(t) \cdot v_{sun_2}(t) > . \end{aligned}$$

The other terms become zero since they are independent each other. The term at the right hand side without G_1 and G_2 is what we want to derive. The heart of calibration is to eliminate these time varying conversion factors.

The conversion factor can be derived using the following measurements,

$$P_{sun_{ii}} \equiv < V^2_{sun_i}(t) > = G_i^2[< v^2_{sun_i}(t) > + < v^2_{n_i}(t) >].$$

In order to get rid of the contribution from noise, we need to measure the output voltage toward blank sky, i.e.,

$$V_{sky_i}(t) = G_i v_{n_i}(t)$$

and

$$P_{sky_{ii}} \equiv < V^2_{sky_i}(t) > = G_i^2 < v^2_{n_i}(t) > .$$

Then,

$$P_{sun_{ii}} - P_{sky_{ii}} = G_i^2 < v^2_{sun_i}(t) > .$$

Finally the following operation,

$$\frac{P_{sun_{12}}}{\sqrt{P_{sun_{11}} - P_{sky_{11}}}\sqrt{P_{sun_{22}} - P_{sky_{22}}}}$$

gives the normalized visibilities.

V. RESULTS

Fig. 5 shows the visibility amplitude derived in this way as a function of baseline length. The visibility amplitude decreases and then increases a little as the baseline is longer. The measurement accuracy is better than 2 %. As expected, the sun is resolved out due to its size for longer baseline.

Assuming disk-like brightness distribution with a diameter of θ_0, we can calculate the visibility function as a function of baseline. They are actually Fourier transformation pairs. In the figure, we plot the eye-fitted visibility curve that is obtained for $\theta_0 = 30'$. The observed data points are in general agreements with the curve except for the longest baseline and the size estimation is also reasonable.

Since limb brightening has been known for the sun at 21 cm, we may be able to fit better using this brightness distribution models (Rohlfs and Wilson 2000). The dotted line in the figure is the best-fit visibility amplitude when the brighter limb is taken into account, where the diameter of disk is $\theta_0 = 28'$ and the inner and outer diameters of limb are $24'$ and $28'$, respectively. In this model, the limb is brighter than the disk area by a factor of 2. As shown in the figure, agreement looks a bit better. There is still disagreement, but some local activities at the solar disk may be responsible for these.

From this experiment, we are confident that the semi-VLBI system works nicely and the measured visibility amplitude is consistent with previous observations. However, we derived radial brightness distribution only, since we played only with the amplitude of visibility. If we could measure the phase as well, we would be able to make full two-dimensional images.

VI. DISCUSSION AND SUMMARY

For science research and educational purpose, we developed a two-element semi-VLBI system. After fringe

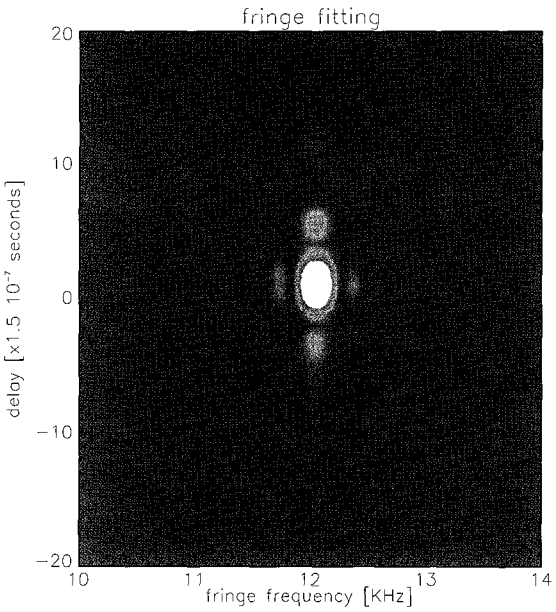

Fig. 4.— Fringe amplitude is displayed as a function of fringe frequency and delays, which is actually the Fourier transformation of Fig. 3.

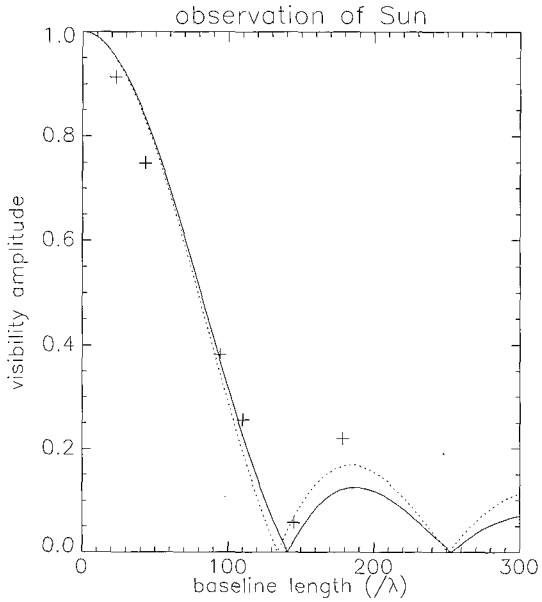

Fig. 5.— Visibility amplitude is shown for various baseline lengths. Crosses are observed points and lines are the eye-fitted visibility amplitude calculated for disk only (solid line) and disk with brighter limb (dotted one). See text for model parameters.

fitting, we succeeded in detecting visibility and in measuring its variation along with baseline length. By fitting the observed data points to the theoretical visibility function derived from the limb-brightened solar disk model, we estimate the size of the sun at 21 cm of $28' - 30'$.

Since this system does not share a common LO and correlation is conducted by software, the system is very close to modern VLBI. Things to be implemented further for complete modernity are (1) for two or hopefully more telescopes to share a high precision reference oscillator, in order to make it possible to measure not only amplitude but also phase of visibility function, and (2) to record data independently but synchronously. By installing GPS-based frequency standard to each antenna, we can accomplish these improvements for the realization of modern VLBI. With this configuration, we could get full information on visibility function to derive two-dimensional images of astronomical sources.

Small aperture and short integration time are the main draw back of this system, restricting observable targets to Sun and several bright supernova remnants (http://haystack.mit.edu/undergrad/srt/index.html). However, even monitoring the sun only will be of great importance, since it is one of the brightest radio variable stars, but not continuously monitored at 1.4 GHz, despite the possibility of discoverying new phenomena. In this respect, it will be really intriguing to develope a VLBI system consisting of several elements and to make routine observations toward Sun and possibly other celestial objects.

ACKNOWLEDGEMENTS

This work was supported by 2005 R&E Program of Ministry of Science and Technology.

REFERENCES

Bastian, T. S., 1991, Solar Microbursts at 1.4 GHz, ApJ, 370, L49

Rohlfs, K. & Wilson, T. L., 2000, Tools of Radio Astronomy, Springer-Verlag

Thompson, A. R., Moran, J. M., & Swenson, G. W., 1986, Interferometry and Synthesis in Radio Astronomy, John Wiley & Sons

Zensus, J. A., Diamond, P. J., & Napier, P. J., 1995, Very Long Baseline Interferometry and the VLBA, Astronomical Society of the Pacific